An Improved Genetic Algorithm for Optimizing EBG Structure With Ultra-Wideband SSN Suppression Performance of Mixed Signal Systems

HAORAN ZHU [1,2], **(Senior Member, IEEE), JIABAO WANG** [1],
YUFA SUN [1], **AND XIAN-LIANG WU** [1], **(Member, IEEE)**

[1]Key Lab of Intelligent Computing and Signal Processing, Ministry of Education, Anhui University, Hefei 230039, China
[2]State Key Laboratory of Millimeter Waves, Southeast University, Nanjing 210096, China

Corresponding author: Haoran Zhu (hrzhu86@gmail.com)

ABSTRACT In this paper, an improved genetic algorithm (GA) for automatically optimizing electromagnetic bandgap (EBG) structure with good power integrity performance is presented. The traditional GA is improved in several ways including Hamming Distance initialization, elite selection and non-repeating crossover, which can generate initial population charactering solution space in detail, increase crossover efficiency, and accelerate convergence. Furthermore, an EBG structure for power distribution network is optimized with the presented GA method to improve the performances of power integrity. The simultaneous switching noise propagation can be prohibited from 0.38 GHz to 20 GHz with a suppression level of -60 dB. Good agreements between the measured results and the simulation ones are observed.

INDEX TERMS Automatic optimization, electromagnetic band gap, genetic algorithm, multi objective optimization, simultaneously switching noise.

I. INTRODUCTION

In the design of high speed mixed signal circuit systems, the optimization method is usually employed to achieve the best value of the structure parameters [1], [2]. However, the optimization of high frequency circuit is usually nonlinear, discontinuous, and non-differentiable, which causes the deterministic method to become time-consuming. Therefore, it is imperative to investigate the intelligent optimization methods that can assistant the circuit design more conveniently [3].

Among the different optimization methods, the most representative one is genetic algorithm (GA), which is generated by simulating the genetics and evolutions of the natural environment [3]. It has been extensively explored as a global optimization algorithm. Considering the difficulty in selecting crossover and mutation probability of GA, adaptive genetic algorithm is presented [4]. In [5], the parallel

genetic algorithm is investigated to save optimization time. Moreover, the multi-objective GAs are researched, such as rank-density based genetic algorithm [6] and nondominated sorting genetic algorithm II [7]. Furthermore, GA is also combined with other optimization algorithms, such as artificial neural network and simulated annealing algorithm [8].

With inherent properties of simplicity, versatility and robustness, GA has also been employed in the field of electromagnetic engineering such as the design of antenna design [9], thinned array [10], microwave imaging [11], frequency selective surfaces [12] and filter [13]. In addition, GA technique is also employed in the power integrity (PI) problems, such as optimizing the selection and placement of decoupling capacitors in the power distribution network (PDN) structure [14]. Moreover, in [15], [16], the dimensions of the electromagnetic bandgap (EBG) structure for suppressing simultaneous switching noise (SSN) is optimized by GA. However, the optimization results of the algorithm show poor performance in terms of frequency band and suppression depth. Therefore, it is important to improve the performance

The associate editor coordinating the review of this manuscript and approving it for publication was Flavia Grassi.

of the conventional GA, which can enable the EBG structure design with good SSN mitigation performance to be more automatically.

In this paper, several improvements are reasonably packaged into improved GA for considering optimizing electromagnetic problem, including Hamming Distance initialization [17], elite selection [18] and non-repeating crossover. An EBG structure with nonbianisotropic complementary split ring resonator (NBCSRR) proposed in [19] as a test structure is optimized automatically with the improved GA. The designed EBG structure can achieve an ultra-wideband SSN suppression performance from 0.38 GHz to 20 GHz with a steep suppression level of −60 dB. Furthermore, the effectiveness of improvements on the simple GA have also been verified.

The outline of the paper is organized as follows. In section II, the work flow chart, several improvement measures, and test functions of the improved GA are discussed. In Section III, the parameter settings of the improved GA and the parameters of EBG structure involved in the optimization design are described. In Section IV, the performances of EBG structure optimized by GA are discussed. Meanwhile, the effectiveness of each improvement is analyzed. Moreover, a sample EBG structure circuit is fabricated and measured to verify the proposed method. Finally, some conclusions are obtained in Section V.

II. DESCRIPTION AND ANALYSIS OF THE IMPROVED GENETIC ALGORITHM
A. DESCRIPTION OF THE IMPROVED GENETIC ALGORITHM

Generally, basic GA is available to solve many problems, especially in the field of multi-parameter and nonlinear optimization. However, it also has some shortcomings, such as the immature convergence of the algorithm and plenty of iterations for convergence. Therefore, some measures are employed to improve the performance of the basic GA. In this paper, several improvements are reasonably packaged into improved GA to improve the convergence speed and precision.

In Fig. 1, the flow chart of the improved genetic algorithm is depicted. The population that generated by Hamming Distance initialization method is initialized with the starting of the algorithm [17]. After calculating the fitness, the individuals in the population are selected, crossed, and mutated to generate new individuals. Then, a novel population is generated and iterated until the optimal solution is found or the maximum generation is reached. It should be noticed that selection operation is set as elite individual protection mechanism [18] and crossover operation uses non-repetitive crossover method in the improved GA. The specific improvements of each module will be described as below.

Firstly, the Hamming Distance initialization is employed to instead the random initialization in the improved GA. Generally, the initial population consists of several individuals, each of them is a string of binary numbers. The size
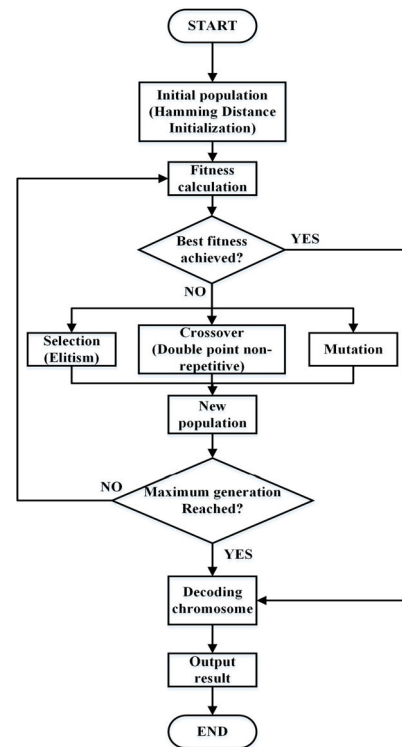

FIGURE 1. The flow chart of improved genetic algorithm.

of population N and the length of chromosome L are determined in advance. If the range of the parameter x involved in optimization is $[a_j, b_j]$ and keeps decimals n, the length of chromosome m_j can be calculated by:

$$2^{m_j-1} < (b_j - a_j) \times 10^n \leq 2^{m_j} - 1 \qquad (1)$$

The length of chromosome L is the sum of the single length of chromosome required for each parameter, which can be calculated by:

$$L = \sum_{j=1}^{n} m_j \qquad (2)$$

Usually, Hamming Distance $H(S_i, S_j)$ between two strings of equal length is the number of positions at which the corresponding different symbols. For the improved GA, Hamming Distance among different individuals in the population is required to be larger than a minimum set value. Supposing the size of the population is N and the length of chromosome is L, the minimum Hamming Distance D can be expressed as:

$$D \leq 2L - N + 1 \qquad (3)$$

In this case, the initial population can be dispersed as much as possible without losing randomness. The improved GA can achieve the goal of scientifically characterizing solution space with a limited number of individuals.

Fig. 2 shows the flow chart of Hamming distance initialization. Firstly, an individual is randomly generated and added to the initial population. Secondly, the Hamming Distance is calculated between the latest generated individual and the
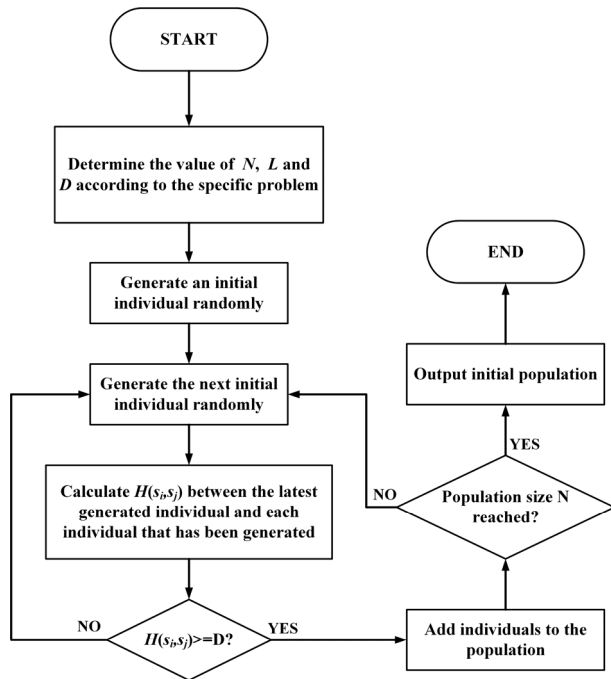
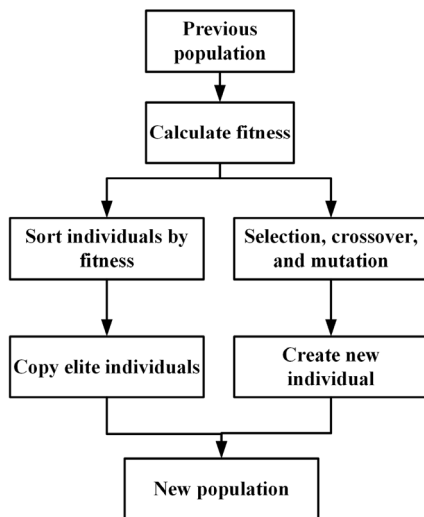**FIGURE 2.** The flow chart of Hamming Distance initialization.

FIGURE 3. The flow chart of elite individual protection mechanism.

other individuals in the population. If the Hamming Distances are all larger than D, the specific individual is put into the population. Otherwise, the above steps are repeated until the population size N is met. Finally, the initial population is generated.

After the population initialization, the selection operation is set as elite individual protection mechanism in the improved GA. From Fig. 3, the flow chart of the elite individual protection mechanism is shown. According to the results of fitness value ranking, the top ranked individuals are treated as elite individuals and directly copied into the next generation before selection. Then, all individuals in the previous population are selected, crossed, and mutated to produce new individuals. In other words, a new population
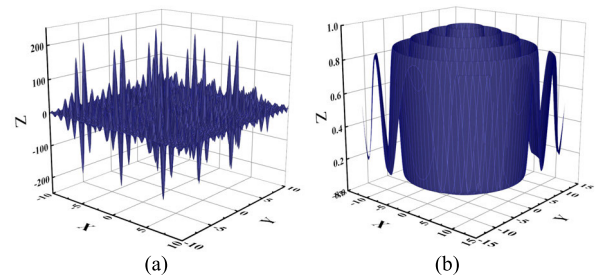

FIGURE 4. 3-D image of testing function: (a) *Shubert*, and (b) *Schaffer*.

is formed based on the previous elite individuals and newly generated individuals. Thus, the loss of the optimal individual in the basic GA is avoided, which accelerates the convergence speed of the algorithm.

Subsequently, non-repetitive double point crossover is employed for the improved GA. From the point of ability to generate new individuals, crossover operation is a primary way to determine the global search capability of the algorithm. However, for the basic GA, the crossover operator has limitations. In the later stages of the algorithm, there are many elite individuals in the population which may have lots of same genetic segments because they may be inherited from the same parents. Under such circumstance, if the gene segments involved in the crossover operation are the same and the algorithm does not judge, the crossover will become meaningless as no new individuals is produced. Therefore, the improved GA judges whether the gene segments involved in crossover are identical. If they are the same, algorithm reselects the gene segments until they are different. Then, the crossover will be executed. Meanwhile, the single-point crossover of the basic GA is changed to double-point crossover for adapting to the multi-parameter optimization.

B. TEST RESULTS OF THE IMPROVED GA
In order to verify the overall effectiveness of the improvements to simple GA, the function *Shubert* and function *Schaffer* are employed for testing, separately.

Shubert function can be described as:

$$F(x, y) = \sum_{i=1}^{5} i\cos[(i+1)x + i] \cdot \sum_{i=1}^{5} \cos[(i+1)y + i] \quad (4)$$

where x and y are independent variables whose domain of definition are both $[-10, 10]$.

As shown in Fig. 4(a), the *Shubert* is a typical multi-peak function with 760 extreme points within the domain of definition, 18 of which are global minimum points of $F(x, y) = -186.731$. Because the gradient of *Shubert* changes dramatically near the extreme point, if the local search ability of is insufficient, it is easy to converge to the local minimum trap $F(x, y) = -186.34$. Thus, *Shubert* is often used to test the ability of optimization algorithms.

As shown in Fig. 5(a), only 26 generations are required to get a global optimal value '-186.7306' for the improved GA. However, the simple GA fell into the trap of local minimums in the 52nd generation. Then, due to the absence of elite
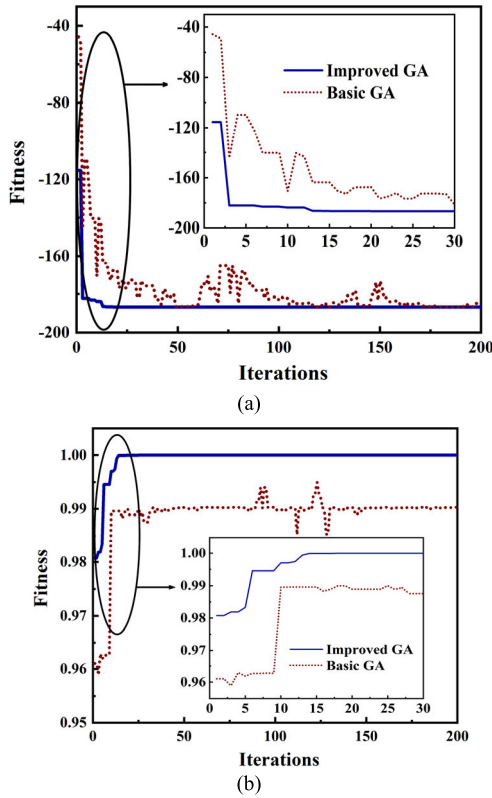
FIGURE 5. The minimum convergence curve of improved-GA and Basic-GA for the testing function of: (a) *Shubert*, and (b) *Schaffer*.

TABLE 1. Comparisons between the improved GA and the simple GA.

Test function	Algorithm	success rate	mean iterations	variance	average convergence time (s)
Shubert	Improved GA	100%	29.24	46.01	0.1117
	Simple GA	30%	504.43	78329	0.5758
Schaffer	Improved GA	46%	92.30	33569	0.6301
	Simple GA	23%	441.17	107750	1.1584

individual protection mechanism, the population begins to degenerate. Until the 181st generation, the simple GA broke through the local optimal solution and found $F(x, y) = 186.7013$, which is located near the global optimal solution and is also the optimal solution that the simple GA can find. It can be obviously discovered that the speed and accuracy of improved GA for optimization are both better than the simple GA. Meanwhile, if the optimal solution is about to find several times, the optimal individual would be destroyed in the next generation. This is also reflected the effectiveness of the elite individual protection mechanism. Therefore, it can be stated that the Hamming distance initialization is more scientific than random initialization.

Moreover, improved GA is also tested by *Schaffer* function, which can be described as:

$$F(x, y) = \frac{1}{2} - \frac{\sin^2 \sqrt{x^2 + y^2}}{[1 + 0.001(x^2 + y^2)]^2} \qquad (5)$$

where x and y are independent variables whose domain of definition are both $[-12.8, 12.8]$.

As shown in Fig. 4(b), Schaffer function has a global maximum $F(0, 0) = 1$ in its domain. Schaffer function is often used to test the effectiveness of the algorithm because there is a circle of global sub-optimal values $F(x, y) = 0.99028$ around the maximum point. If the local search ability of the algorithm is weak, it is easy to converge to the global sub-optimal value. From Fig. 5(b), the improved GA converges

to the global optimal solution after 15 iterations. However, the basic GA can only converge to the global sub-optimal value. During the iteration, the algorithm repeatedly discovers individuals who exceed the global suboptimal value. However, individuals are quickly destroyed without elite individual protection in the basic GA.

In order to verify the effectiveness of the improved GA in detail, function Shubert and Schaffer are employed for testing the convergence speed and precision. Improved GA and simple GA are used to search the maximum or minimum values of two test functions. Then, the search results of the different GA approaches in 100 trials for each test function are counted. For Shubert, the flag of success is that the minimum value sought by GA is less than -181.7308. For Schaffer, the flag of success is that the maximum value sought by GA is larger than 0.999. Finally, the calculating results, including success rate of the search, the average number of iterations, the variance and the average convergence time, are listed in Table 1 for comparison.

From TABLE 1, after adding the Hamming distance initialization, elitism selection and non-repetitive double point crossover to the simple GA, the success rate for searching the most value is greatly improved. Meanwhile, the number of iterations and convergence time required for convergence are also reduced. Taking the results of the testing function Schaffer for example, the success rate of the improved GA for searching the global maximum value is 46 %. Compared to the simple GA, the success rate has doubled. The average number of convergence iterations has also decreased significantly.

III. ANALYSIS OF THE IMPROVED GA FOR OPTIMIZED EBG STRUCTURE WITH CSRR

From the above analysis in section II, the conventional GA is improved in several ways to increase the convergence speed and precision. In order to verify the effectiveness of the improved GA method, an EBG structure is automatically designed for ultra-wideband mitigation of SSN in high-speed circuit.

With the increase of circuit integration and clock frequency, SSN has become a huge obstacle in the mixed signal system. It is necessary and significant to reduce the SSN coupling with a wide stopband and steep suppression level.
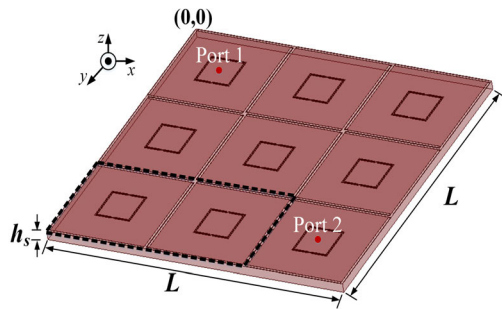
FIGURE 6. 3-D view of the initial power plane composed by array of 3 × 3 EBG structure.
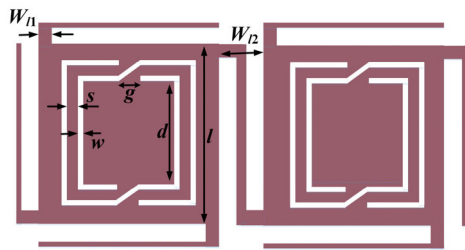

FIGURE 7. Top view of two adjacent EBG units connected with L-bridge and corresponding parameters.

EBG structure, with an inherent property of bandstop filter, is widely employed in the field of SSN mitigation [20]. In this paper, in order to verify the ability of improved GA to optimize PI issues, the EBG structure proposed in [19] is treated as the test structure.

A. DESCRIPTION OF THE EBG STRUCTURE

From Fig. 6, the initial power plane is composed of 3 × 3 EBG structures while the ground plane is continuous. The power and ground layer are made of copper which have a thickness of 0.035 mm. Noise sources and noise sensitive devices are placed on port 1 and port 2, respectively. L and h_s represent the side length of the texting board and the thickness of the substrate, respectively. The length of L is determined by the optimization result while h_s is equal to 0.2 mm. The material of the used dielectric substrate is FR-4 with effective permittivity $\varepsilon_r = 4.4$ and loss tangent $tan\delta = 0.02$.

Fig. 7 shows the top view of EBG structures of NBCSRR in the black dotted frame of Fig. 6. The L-bridge is used to connect two adjacent EBG units, where w_{l2} represents the distance between two EBG units and w_{l1} is the width of the L-bridge. Notation l is the width of pad and d is the inner length of NBCSRR structure. Meanwhile, notation g is the length of split while w and s represent the width of split ring and the width of conductor in CSRR, respectively.

B. SETTING VALUES OF THE IMPROVED GA AND OPTIMIZED PARAMETERS OF THE EBG STRUCTURE

In order to describe the optimization procedure of EBG structure in detail, the setting values and optimized parameters of the improved GA method is introduced.

TABLE 2. Parameters of EBG structure involved in optimization.

Parameter	Range (mm)	Precision (mm)	Chromosome length
d	[5,28]	0.1	8
s and w	[0.1,0.5]	0.01	6
w_{l1}	[0.2,0.5]	0.01	6
w_{l2}	[0.8,1.2]	0.01	6

TABLE 3. Setting values of the improved GA.

Elite rate	10%
Population size	20
Maximum iteration	20
The length of chromosome	32 (8+6+6+6)
Minimum Hamming distance	45

1) OPTIMIZATION PARAMETERS OF THE EBG STRUCTURE

According to formula (1), if the optimized parameter has a big range of values, a larger chromosome length is required to ensure the accuracy in the process of encoding and decoding. Therefore, based on the trade-off between the precision and range of parameter, variables s, w, w_{l1} and w_{l2} retain two decimals while d keeps one decimal. Moreover, the length of overall chromosome including all parameters are set as 32, which is the sum of the length of chromosome of each parameter calculated by formula (1) and (2). Finally, the optimization range and precision of parameters is listed in TABLE 2.

2) SETTING VALUES OF THE GA

Firstly, 10% of individuals with higher fitness value are treated as elite individual that can be copied directly to the next generation. Moreover, the number of individuals in population and the maximum number of iterations are both set as 20 for the consideration of efficiency and accuracy. In addition, the minimum Hamming Distance between individuals is set to 45 according to formula (3). According to the above analysis, the final setting values of the improved GA are summarized in TABLE 3.

3) FITNESS FUNCTION

Fitness is used to assess the performance of individuals in population. GA determines the probability that each individual in the current population inherited to the next generation population according to the probability proportional to the fitness of the individual. Therefore, according to different types of problems, it is necessary to predetermine the conversion rules from the performance of individuals to the fitness value.

Generally, The PDN can be regarded to effectively suppress the SSN when the transmission response of the PDN is less than −30 dB [20]. In other words, if the suppression level $|S_{21}|$ is larger than −30 dB, the sampling point has no contribution to the overall fitness of the individual. Therefore, the corresponding fitness is set to 0. Then, for parts below
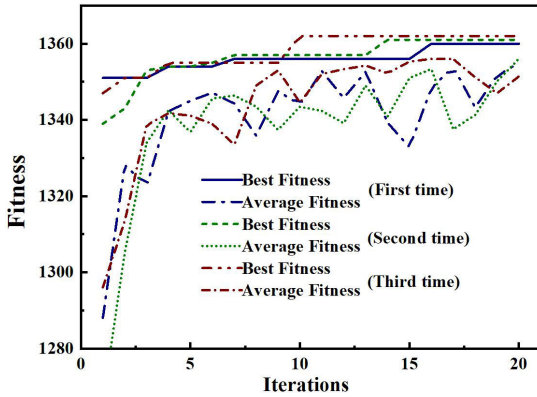
FIGURE 8. Best fitness line and average fitness line of improved GA in three independent experiments.

FIGURE 9. Best fitness line and average fitness line of simple GA in three independent experiments.

−30 dB, different weights are assigned for sampling points according to different suppression levels, so that the fitness value has a degree of discrimination. Thus, the corresponding fitness function employed in the improved GA is expressed as:

$$fit_i = \begin{cases} 0, & S_{21} > -30dB \\ 5, & -40dB < S_{21} \le -30dB \\ 6, & -50dB < S_{21} \le -40dB \\ 7, & S_{21} \le -50dB \end{cases}$$

$$Fitness = \sum_{i=0}^{n} fit_i \qquad (6)$$

where f_{iti} and $|S_{21}|$ are the fitness value and the insertion loss of the sampling frequency, respectively. Notation n represents the number of sampling points for the transmission response.

C. SIMULATED RESULTS OF THE BASIC GA AND THE IMPROVED GA

Based on the above analysis of setting values of the improved GA and optimization parameters of the EBG structure, an EBG structure with NBCSRR is optimized by improved GA for wideband SSN mitigation with a steep suppression level. Meanwhile, the optimization of the EBG structure is also used as a test method to verify the effectiveness of improved GA for PI issues. The basic GA and improved GA are utilized to optimize the EBG structure shown in Fig. 6. Two hundred samples of S_{21} data that simulated by Ansys High Frequency Structure Simulator (HFSS) are used to calculate the fitness value. However, because the 3D full-wave electromagnetic simulation is a time-consuming process, in order to save the simulation time in the stage of using GA method for optimization EBG structure, the range of the optimization frequency is set from 50 MHz to 10 GHz.

Best fitness and average fitness line of improved GA for optimizing EBG structure are shown in Fig. 8. From the figure, three optimizations performed by improved GA achieve convergence at the end of algorithm iteration. The average convergence generation and the average best fitness value are
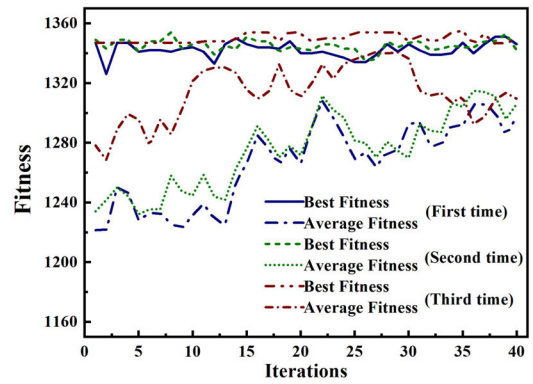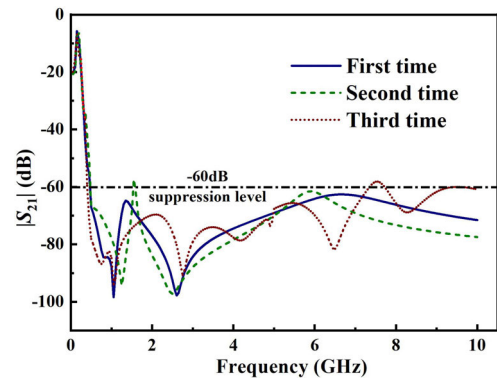

FIGURE 10. Simulated transmission coefficients of individuals with the best fitness in three improved GA experiments.

13.33 and 1361, respectively. In addition, the average fitness value of the population increases rapidly in the former five generations, while the average fitness is close to the best fitness of each generation in the later period of iteration. This means that the focus of improved GA is changed from global optimization to local optimization.

Fig. 9 shows the convergence line and average fitness line of simple GA. From the figure, which is different from improved GA is that convergence was not achieved in all three experiments after 40 iterations. It can be discovered that due to the lack of elitism mechanism, the reorganization of individuals who performed well in the previous generation often occurred, leading to the degradation of the overall performance of the population. Then, the average fitness of each optimal individual is 1353.33, which is worse than the optimized individual of improved GA. The average fitness value of the population is in a slowly increasing state. This is quite different from the average fitness curve of improved GA, which means that the evolution of simple GA is slow.

After decoding the chromosome of the best fitness individual, the corresponding parameters of the EBG structure optimized by the improved GA are presented in Table 4. Fig. 10 shows the transmission coefficients of the EBG structure formed by the parameters corresponding to the optimal

TABLE 4. The structure parameters optimized by the improved GA.

Parameter	First time Value (mm)	Second time Value (mm)	Third time Value (mm)
d	7.35	6.62	8.25
s	0.49	0.16	0.11
w	0.15	0.21	0.18
w_{l1}	0.21	0.23	0.21
w_{l2}	1.38	1.21	1.17

TABLE 5. The structure parameters optimized by the simple GA.

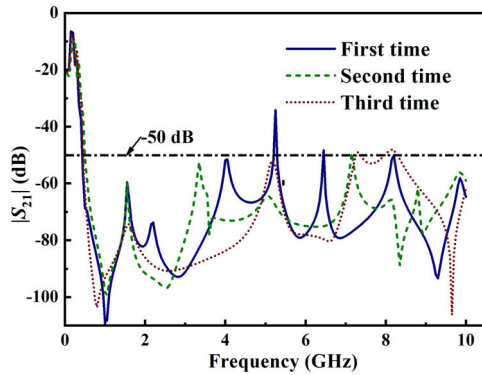| Parameter	First time Value (mm)	Second time Value (mm)	Third time Value (mm)
d	9.33	9.33	10.86
s	0.31	0.31	0.12
w	0.21	0.20	0.13
w_{l1}	0.21	0.39	0.41
w_{l2}	1.32	1.32	1.39

FIGURE 11. Simulated transmission coefficients of individuals with the best fitness in three simple GA experiments.
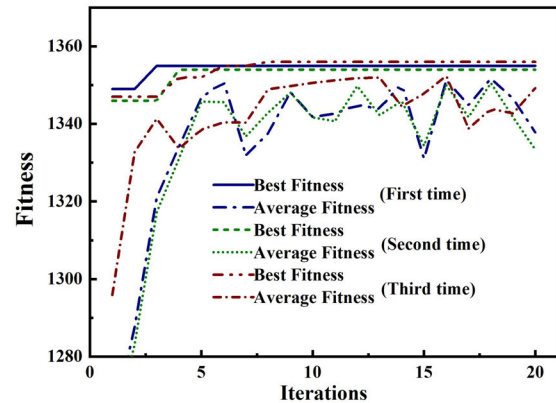

FIGURE 12. Best fitness line and average fitness line of incomplete improved GA without Hamming distance initialization in three independent experiments.

fitness value of the improved GA. Taking the third optimization result as an example, improved GA converges to 1362 in the 10th generation. From the figure, the SSN propagation between port 1 and port 2 can be prohibited from 0.45 to 10 GHz under the suppression level of -60 dB. Good optimization performances are also achieved with the other two independent experiments.

Then, the corresponding parameters of the EBG structure optimized by simple GA are decoded and presented in III-D. As can be seen from Fig. 11, the simulated $|S_{21}|$ curves of best individual of simple GA in three experiments are depicted. Compared with the corresponding results of the improved GA shown in Fig. 10, the rejection level of the simple GA is not good with lots of anti-resonances in the suppression band. It is because that in comparison the improved GA, the simple GA cannot easily find the maximum fitness value and converges to a smaller fitness value with a setting maximum iteration number of 40 in the experiment, which is also verified in Table 1. Thus, the noise rejection level cannot be reduced entirely with the designed EBG structures, which is optimized with the simple GA of small fitness value.

By comparing the results of the two GA method, the performances of the improved GA are significantly better than the simple GA in terms of convergence speed and stability. Moreover, the improved GA can effectively suppress the anti-resonance of the EBG structure and increase the noise suppression level.

D. INFLUENCE FOR THE IMPROVEMENTS OF THE GA

After researching the overall performance of improved GA, the impact of each improvement on the simple GA is explored one by one in this subsection. Comparing the incomplete improved GA which misses one improvement to the full version improved GA, the influence of this improvement can be discussed.

1) WITHOUT HAMMING DISTANCE INITIALIZAION

Three independent experiments are performed by incomplete improved GA which misses Hamming Distance initialization. Convergence line and average fitness line are shown in Fig. 12. The algorithm converges to 1355 after 4.5 iterations on average who seems to converge much faster than the complete improved GA. In fact, the algorithm in three experiments are all caught in premature which means that the algorithm stop evolution too early and cannot find the global optimal solution. The reason for this situation is that the randomly initialized population may not contain the information of the optimal solution or the population is clustered in a small range. Thus, from the comparison results, the initial population generated by Hamming distance initialization can be dispersed as much as possible without losing randomness, ensuring the improved GA avoids premature traps.

2) WITHOUT ELITE INDIVIDUALS PROTECTION MECHANISM

Fig. 13 shows the result of optimization using incomplete improved-GA without elite individual protection mechanism. The algorithm which does not achieve convergence until the maximum number of iterations. The average fitness of the first and second trials has a slow upward trend. Furthermore, the average fitness of the third experiment have a huge drop
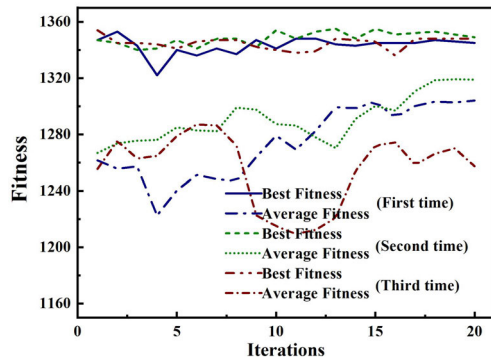
FIGURE 13. Best fitness line and average fitness line of incomplete improved GA without elite individual protection mechanism in three independent experiments.
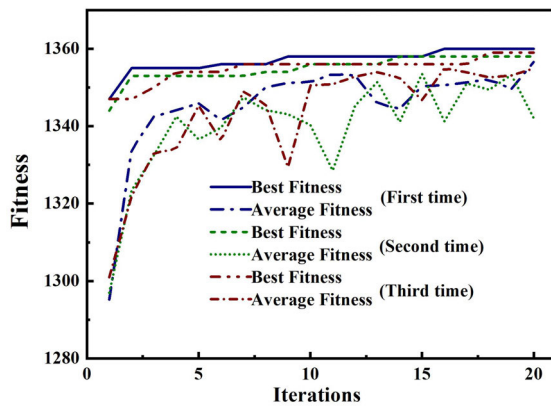

FIGURE 14. Best fitness line and average fitness line of incomplete improved GA without non-repetitive crossover in three independent experiments.

FIGURE 15. Best fitness line and average fitness line of improved GA whose optimized frequency band is from 50 MHz to 20 GHz.

TABLE 6. Optimized value of parameters involved in design.

Parameter	Value(mm)	Parameter	Value(mm)
d	5.36	w_{l1}	0.38
S	0.49	w_{l2}	0.90
w	0.37	-	-
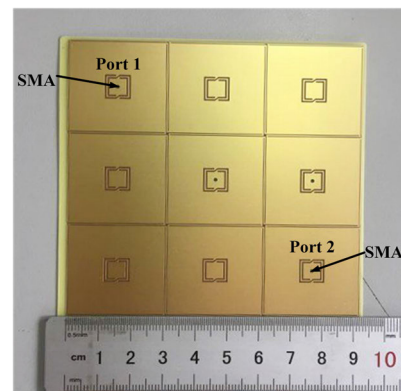
FIGURE 16. Photograph of the fabricated board.

in the 7th generation, which indicated that the excellent genes in the population were seriously damaged in this genetic recombination, resulting in population degradation. This phenomenon illustrates that the GA using elite mechanism can speed up convergence without destroying the excellent individuals.

3) WITHOUT NON-REPETITIVE CROSSOVER

An incomplete improved GA is executed to illustrate the effect of non-repetitive crossover. Fig. 14 shows the results of three independent optimizations with the algorithm converges to 1358.67 at 16th generation on average. In comparison with the completed improved GA, 3 generations are slower with the incomplete improved GA. This means that the crossover operator improvement for simple GA can accelerate the optimization of the algorithm.

IV. SIMULATED AND MEASURED SSN SUPPRESSION RESULTS OF THE EBG STRUCTURE OPTIMIZED BY IMPROVED GA

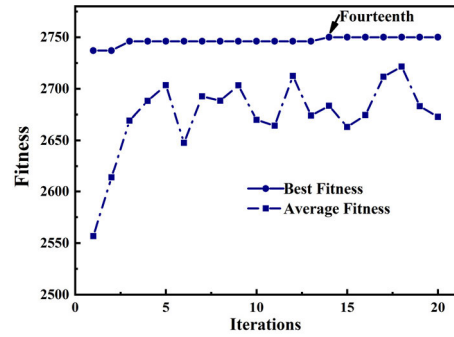Based on the above analysis, several measures are conducted on the simple GA, including Hamming distance

initialization, non-repetitive crossover, and elite individual protection mechanism. The proposed improved GA can generate initial population charactering solution space in detail, increase crossover efficiency and accelerate convergence at the same time.

Furthermore, the presented GA is employed to optimize the noise mitigation performance of the EBG structure which is shown in Fig. 6. In order to obtain the SSN suppression performance within a wide frequency band, the simulation frequency band is set to 0-20 GHz and 2000 frequency points for calculating fitness values are sampled from the simulated transmission coefficient data. From Fig. 15, improved GA converges to 2750 in the 14th generation. After decoding the chromosome of individual with maximum fitness, the optimized parameters are given in TABLE 6.

As shown in Fig. 16, according to the optimized result, a testing board is designed to verify the definiteness of the simulation and improved GA. The sample circuit is fabricated
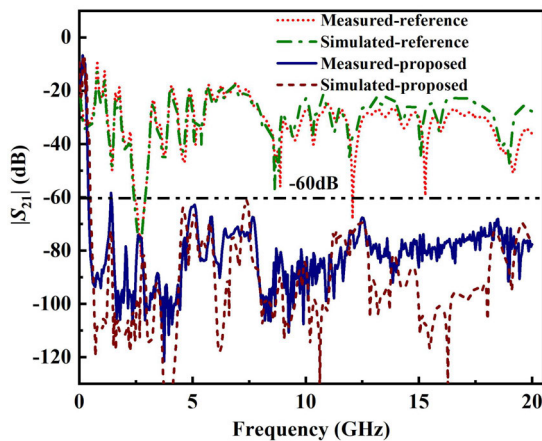
FIGURE 17. Simulated and measured $|S_{21}|$ parameters of the PDN optimized by improved GA in comparison with the corresponding results of reference board.
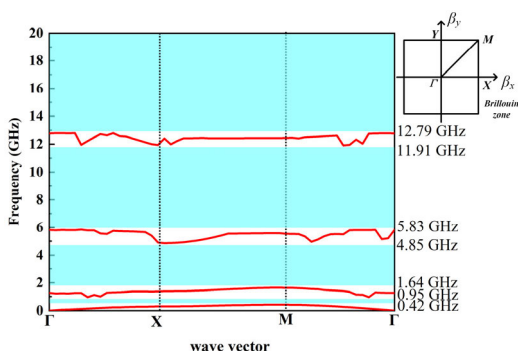

FIGURE 18. 2-D dispersion diagram of the optimized EBG structure.

with the standard printed circuit board technology. Vector network analyzer (VNA) Keysight N5227B is employed to measure the transmission responses of the optimized PDN.

Fig. 17 shows the measured insertion loss of the optimized EBG structure and reference solid board, with the simulated results also given for comparison. The SSN is suppressed significantly with the structure optimized by improved GA. Compared with the reference board, the measured noise mitigation bandwidth of the designed EBG structure is from 0.37 GHz to 20 GHz with a suppression level of −60 dB. It is worth to noticing that the cutoff frequency of −30 dB is 320 MHz. Moreover, the simulation results including the anti-resonance frequencies points agree well with the measurements. Slight discrepancies are observed with the tolerance in the manufacturing process and the dissipation properties of FR-4 substrate.

Furthermore, in order to effectively evaluate the electromagnetic performances of the presented EBG structure, the 2-D dispersion diagram is also depicted to describe the transmission behaviors of the periodic structure within a wide frequency band. As shown in Fig. 18, a wide stopband from 0.42 GHz to 20 GHz is observed except for some minor passbands. The low frequency passbands near 1 GHz and 5 GHz

are consistent with the anti-resonance frequencies, which are mainly induced with the parasitic parameters of the rectangular cavity EBG structure. In addition, with increasing of the operating frequency, the dielectric loss of the used substrate would enlarge the transmission loss, which is responsible for the generation of the high-frequency passband near 12 GHz.

V. CONCLUSION

An improved genetic algorithm with advantages of rapid convergence and high precision is proposed to solve SI issues in this paper. By comparing the ability of planar EBG structures optimized by simple GA to suppress SSN propagation, the effects of different improvements on GA for optimizing EBG structure are explored. The PDN optimized by improved GA can prohibit the SSN propagation between power and ground planes from 0.38 to 20 GHz with a suppression level of -60 dB. The measurement results are highly consistent with the simulation predictions. Using the improved GA proposed in this paper to optimize the PDN structure, the designer can spend less time on optimization and be freed from repeated debugging. Meanwhile, the performance of optimized PDN structure is better than artificial tuning.

REFERENCES

[1] J. Vasconcelos, R. Saldanha, L. Krahenbuhl, and A. Nicolas, "Genetic algorithm coupled with a deterministic method for optimization in electromagnetics," *IEEE Trans. Magn.*, vol. 33, no. 2, pp. 1860–1863, Mar. 1997.

[2] K. Choi, D.-H. Jang, S.-I. Kang, J.-H. Lee, T.-K. Chung, and H.-S. Kim, "Hybrid algorithm combing genetic algorithm with evolution strategy for antenna design," *IEEE Trans. Magn.*, vol. 52, no. 3, pp. 1–4, Mar. 2016.

[3] R. Haupt, "An introduction to genetic algorithms for electromagnetics," *IEEE Antennas Propag. Mag.*, vol. 37, no. 2, pp. 7–15, Apr. 1995.

[4] M. Srinivas and L. Patnaik, "Adaptive probabilities of crossover and mutation in genetic algorithms," *IEEE Trans. Syst., Man, Cybern.*, vol. 24, no. 4, pp. 656–667, Apr. 1994.

[5] H. Mühlenbein, M. Schomisch, and J. Born, "The parallel genetic algorithm as function optimizer," *Parallel Comput.*, vol. 17, nos. 6–7, pp. 619–632, Sep. 1991.

[6] H. Lu and G. Yen, "Rank-density-based multiobjective genetic algorithm and benchmark test function study," *IEEE Trans. Evol. Comput.*, vol. 7, no. 4, pp. 325–343, Aug. 2003.

[7] K. Deb, A. Pratap, S. Agarwal, and T. Meyarivan, "A fast and elitist multiobjective genetic algorithm: NSGA-II," *IEEE Trans. Evol. Comput.*, vol. 6, no. 2, pp. 182–197, Apr. 2002.

[8] S. W. Mahfoud and D. E. Goldberg, "Parallel recombinative simulated annealing: A genetic algorithm," *Parallel Computing*, vol. 21, no. 1, pp. 1–28, Jan. 1995.

[9] F. Villegas, T. Cwik, Y. Rahmat-Samii, and M. Manteghi, "A parallel electromagnetic genetic-algorithm optimization (EGO) application for patch antenna design," *IEEE Trans. Antennas Propag.*, vol. 52, no. 9, pp. 2424–2435, Sep. 2004.

[10] R. Haupt, "Thinned arrays using genetic algorithms," *IEEE Trans. Antennas Propag.*, vol. 42, no. 7, pp. 993–999, Jul. 1994.

[11] S. Caorsi, A. Costa, and M. Pastorino, "Microwave imaging within the second-order Born approximation: Stochastic optimization by a genetic algorithm," *IEEE Trans. Antennas Propag.*, vol. 49, no. 1, pp. 22–31, Jan. 2001.

[12] J. Bossard, D. Werner, T. Mayer, and R. Drupp, "A novel design methodology for reconfigurable frequency selective surfaces using genetic algorithms," *IEEE Trans. Antennas Propag.*, vol. 53, no. 4, pp. 1390–1400, Apr. 2005.

[13] N. Venkatarayalu, T. Ray, and Y.-B. Gan, "Multilayer dielectric filter design using a multiobjective evolutionary algorithm," *IEEE Trans. Antennas Propag.*, vol. 53, no. 11, pp. 3625–3632, Nov. 2005.

[14] I. Erdin and R. Achar, "Multipin optimization method for placement of decoupling capacitors using a genetic algorithm," *IEEE Trans. Electromagn. Compat.*, vol. 60, no. 6, pp. 1662–1669, Dec. 2018.

[15] T. H. Kim, M. Swaminathan, A. E. Engin, and B. J. Yang, "Electromagnetic band gap synthesis using genetic algorithms for mixed signal applications," *IEEE Trans. Adv. Packag.*, vol. 32, no. 1, pp. 13–25, Feb. 2009.

[16] B. Appasani, V. K. Verma, R. Pelluri, and N. Gupta, "Genetic algorithm optimized electromagnetic band gap structure for wide band noise suppression," *Prog. Electromagn. Res.*, vol. 71, pp. 109–115, 2017.

[17] G. Rudolph, "Convergence analysis of canonical genetic algorithms," *IEEE Trans. Neural Netw.*, vol. 5, no. 1, pp. 96–101, Jan. 1994.

[18] D. Bhandari, C. A. Murthy, and S. K. Pal, "Genetic algorithm with elitism model and its comvergence," *Int. J. Pattern Recognit. Artif. Intell.*, vol. 10, no. 06, pp. 731–747, Sep. 1996.

[19] H.-R. Zhu and J.-F. Mao, "Localized planar EBG structure of CSRR for ultrawideband SSN mitigation and signal integrity improvement in mixed-signal systems," *IEEE Trans. Compon., Packag. Manufact. Technol.*, vol. 3, no. 12, pp. 2092–2100, Dec. 2013.

[20] T.-L. Wu, Y.-H. Lin, and S.-T. Chen, "A novel power planes with low radiation and broadband suppression of ground bounce noise using photonic bandgap structures," *IEEE Microw. Wireless Compon. Lett.*, vol. 14, no. 7, pp. 337–339, Jul. 2004.
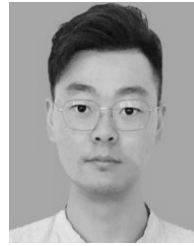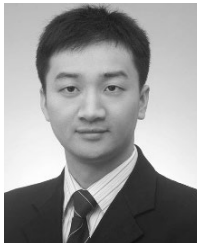
JIABAO WANG was born in 1994. He received the B.S. degree in electronic information engineering from Anhui University, Hefei, China, in 2017, where he is currently pursuing M.S. degree in electromagnetic field and microwave technology.

His research interests include the power integrity and signal integrity analysis of high-speed circuit.

YUFA SUN was born in 1966. He received the B.S. and M.S. degrees in radio physics from Shandong University, in 1988 and 1991, respectively, and the Ph.D. degree in electromagnetic field and microwave technology from the University of Science and Technology of China, in 2001.

Since 1991, he has been a Faculty Member with Anhui University, Anhui, China, where he is currently a Professor with the School of Electronics and Information Engineering. He was a Visiting Scholar with the City University of Hong Kong, from 2002 to 2003, and a Postdoctoral Researcher with the University of Science and Technology of China, from 2003 to 2006. His research interests include electromagnetic scattering and target recognition, computational electromagnetics, and antenna theory and technology. He has authored or coauthored more than 130 journal articles.

HAORAN ZHU (Senior Member, IEEE) was born in Anhui, China, in 1986. He received the B.S. degree in electronic engineering from the Anhui University of Technology, China, in 2007, the M.S. degree in electronic engineering from Anhui University, China, in 2010, and the Ph.D. degree in electrical engineering from Shanghai Jiao Tong University, China, in 2014.

From June 2014 to September 2017, he was a Senior Engineer with the Research Department of Micro-System, East China Research Institute of Electronic Engineering, Hefei, China. Since September 2017, he has been an Associate Professor with the School of Electronics and Information Engineering, Anhui University. Since February 2019, he has been a Research Fellow with the Department of Electrical Computing Engineering, National University of Singapore. His recent research interests include the 3D integration technologies of antenna and RF circuit system, signal integrity and power integrity analysis of high speed mixed-signal systems, and miniaturized microwave integrated passive circuit.

XIAN-LIANG WU (Member, IEEE) was born in Bozhou, China, in 1955. He received the B.S. degree in electronic engineering from Anhui University, Hefei, China, in 1982.

He is currently a Full Professor with the Department of Electronic Engineering and the Director of the Laboratory of Electromagnetic Field and Microwave Technology, Anhui University, and the Principal with Hefei Normal University, Hefei. He has authored or coauthored more than 100 articles and three books. His current research interests include electromagnetic field theory, electromagnetic scattering and inverse scattering, and wireless communication. He is a Senior Member of the Chinese Institute of Electronics. He is the Associate Director of the Chinese Electronic Institute of Antenna Propagation and the Chinese Institute of Microwave Measurement.

• • •